Buck-Boost Converter Control for Constant Power Loads in Aeronautical Applications

A. Cavallo, G. Canciello, A. Russo

***Abstract*— The design of control strategies for bidirectional DC/DC converters is proposed. The motivation for this paper is the increased request from aeronautic applications of innovative and "smart" controllers able to manage automatically electrical energy distribution onboard. Two different control strategies are proposed, and also a higher level, supervisory control law is presented, to switch between the two low-level strategies in a safe way, i.e., ensuring the stability of the overall control law. The first low-level controller is based on the definition of a sliding manifold on which the system state evolution is confined by means of High-Gain or Variable Structure Control, while the second low-level controller exploits an adaptive approach to define a suitable reference current. The high-level switching strategy enables the commutation from one low-level controller to the other only if the Region of Attraction of the second controller has been reached, thus ensuring stability of the commutation. The strategies are designed for the case of Constant Power Loads (CPL), that are well known causes of instability. Detailed simulation results in MATLAB/Simulink are provided, in different scenarios, showing the effectiveness of the proposed controllers.**

I. Introduction

The increasing air traffic, the need for weight (and size) reduction and consequent fuel reduction, the request for more reliable devices on board, are all factors motivating the increased interest of the aerospace industry towards the concept of More Electric Aircraft (MEA) [1]. In the last 15 years there has been a great interest of the EU in research projects focussing on different aspects related to MEA, starting with POA [2], going on with the MOET [3], until the very recent CleanSky initiatives [4]. Currently, three major research waves have been spotted, covering a time horizon above 2030's [5]. Basically, the key idea is to replace hydraulic and pneumatic devices with their electric counterpart, e.g., Electro-Magnetic Actuators (EMA).

The possibility of dramatically increase the role of the electric-actuated devices has changed also the concepts of electric power grid, power management and power distribution on-board. One of the first ideas has been to consider, in addition to standard 115VAC networks, traditionally used for commercial loads and 28VDC networks, used for supplying electrical systems onboard, different AC and DC power networks [3]. Specifically, new DC power distribution has been considered, with High Voltage (HV) busses at 270VDC, for small aircraft, or 540VDC, for large aircraft (that, in turn, come from a rectified version of the current from an aeronautic generator [6]). However, since the Low Voltage (LV) bus is still supplied by one or more batteries at 28VDC, possibly with also energy storage devices [7], like supercapacitors, there is the need for DC/DC converters (BBCU's, i.e., Buck-Boost Converter Units) acting as bridges between different DC busbars [8].

Moreover it is apparent that suitable control strategies may be designed to improve the flexibility of the two electric distribution systems (HV and LV systems). For instance, in the event of HV generator overload, the battery can be used as an additional power source, supplying energy to the HV load [9], [10]. This extended use of batteries has a beneficial effect in terms of weight reduction onboard, since it is known [11] that electric generators have the capability to supply current exceeding their nominal (rated) level during a short transient, so that if after this transient another device (e.g., a battery) can supply extra current there is no need for increasing the rated power (and weight) of the generator. As a simple criterion for characterising this phenomenon, in the aeronautic field it is usual to consider the so-called "5 seconds" and "5 minutes" overload capabilities, that are a simplified version of the true overload curve of the generator. Basically, it is assumed that for the first 5 seconds the generator can supply high power (or current) levels, that gradually decrease until an overload level P_{OL} is attained after 5 minutes. Generator sizing is based on P_{OL}, so that if batteries are able to supply power within 5s there is no need to increase the size (and the weight) of the generator. Applications of this approach are found in the aeronautical field [9], [10], [12] or in automotive, with the increased interest for hybrid vehicles [13].

Usually, the overload condition is caused by a load absorbing active power from the electric grid. This load can be modelled as a simple variable resistor [9], [14], to take into account active power. However, in some cases the loads are power controlled devices, i.e., electric machines with a controller embedded such that their power consumption is kept constant in the face of uncertain or time-varying parameters. In such cases the load must be modelled as Constant Power Loads (CPL's).

It is well known the CPL's behave as *negative resistances* [15], and can be the cause of instability [16]. Possible control laws to counteract this effect are proposed in [17], or [18], in the framework of sliding mode control. The stability based on impedance analysis is considered in [19]. See also [20] for an updated review of existing techniques. In this paper, we propose a control approach based on

This work was partially supported by CleanSky2 grant Programme: H2020-CS2-CFP04-2016-02 JTI- CS2-2016-CFP04-REG-01-08 Proposal: 755485 ESTEEM

The authors are with Department of Engineering, University of Campania, 81031 Aversa, Italy {alberto.cavallo, giacomo.canciello, antonio.russo1}@unicampania.it

the definition of a suitable sliding manifold on which the controlled converter has to evolve so that stability is ensured. Moreover, since the focus is not only on the CPL, but on the effect of the CPL in the whole power grid, also the "5s-5min" overload described above has to be taken into account. Thus a strategy for the control of the BBCU *in the presence of CPL* causing overload is presented in this paper. Since the overload/no overload conditions require different controllers, a supervisor must be defined for switching among various strategies. When commuting control *modes*, e.g., control configurations, it is important also to estimate the Region of Attraction (ROA) of each controller. Moreover, it is well known that switching among stabilising controllers may result in instability [21], hence stability of the resulting closed-loop configuration has to be investigated. Some papers have been presented discussing supervisory control of switching systems [22]. Most of the proposed techniques are based on the theory in [23].

In this paper the BBCU is used to recharge the batteries in normal conditions, i.e., when the power requested by all the loads, including the BBCU in buck mode itself, is below a certain threshold. If however an overload occurs, the converter automatically switches to generator current limitation mode, and the battery initially reduces its power request and, if necessary, eventually reverses the power flow, thus helping the generator.

The effectiveness of the proposed control strategy is tested by detailed simulations in MATLAB/Simulink/PowerSim, including switches and electric elements. Two scenarios are investigated, the first one considering nominal conditions first, when the generator recharges the battery with a fixed current, then two overload condition, the second being more severe than the first. In the second scenario, another DC/DC converter is added, acting as another CPL itself. Again, simulations confirm the effectiveness of the strategy.

II. The network model

Although the classical topology of the BBCU control uses just one inductor and one capacitor, in this paper we will refer to a third-order, non-inverting buck-boost topology, as done in [24], [10]. The network schematic is reported in Fig. 1. Here the BBCU has a synchronized switches couple $Q_1 - Q_2$ to be controlled in anti-phase (i.e., Q_1 is on when Q_2 is off, and viceversa).

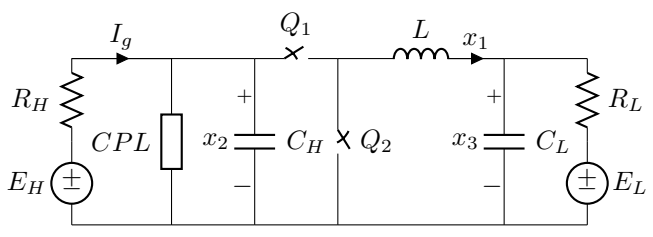

Fig. 1. Bidirectional Buck-Boost converter schematic

The bidirectional converter allows the power to be exchanged between HV and LV sides. E_H represents the aircraft electric generator after rectification, while E_L is a battery. In normal operating condition the generator is assumed to charge the battery at constant current.

Moreover, on the HV side a CPL is considered, that absorbs a constant power P_0 from the network. The value of this power is varied in time, so as to consider different CPL's during BBCU operations.

Moreover, a maximum generator current I_{OL} is considered, that the generator is allowed to exceed only in a short transient (less then 5s). The equations of the converter are easily derived in both configurations (Q_1 on, Q_2 off) and (Q_1 off, Q_2 on), and can be described in a compact way as

$$\dot{x}_1 = -\frac{1}{L}x_3 + \frac{1}{L}x_2 u \tag{1}$$

$$\dot{x}_2 = -\frac{1}{\tau_H}x_2 - \frac{P_0}{C_H x_2} - \frac{1}{C_H}x_1 u + \nu_H \tag{2}$$

$$\dot{x}_3 = \frac{1}{C_L}x_1 - \frac{1}{\tau_L}x_3 + \nu_L \tag{3}$$

where x_1 is the current flowing through the inductor L, x_2 is the voltage on the capacitor C_H on the high-voltage bus side and x_3 is the voltage on the capacitor C_L on the low-voltage bus side, $u \in \{0, 1\}$ is the control, $\tau_i = R_i C_i$ and $\nu_i = E_i/\tau_i$, $i = \{H, L\}$.

III. BBCU Control

Two strategies are presented, with different hierarchy.

A. Current control, LV side

In normal operating conditions, the converter is asked to recharge the battery. This is done by imposing a piecewise-constant set-point $\bar{x}_1$ to the inductor current x_1, i.e., a set-point changing only at a sequence of time instants t_i, $i = 1, ..., N$, for some $n \in \mathbf{N}$, with $t_{i+1} > t_i$. Next, for each time interval $[t_i, t_{i+1}]$, define a sliding manifold

$$\mathcal{S} = \{(x, t) | \sigma_{1i}(t, x_1) = 0, \forall t \in [t_i, t_{i+1}]\} \tag{4}$$

where,

$$\sigma_{1i}(t, x_1) = \bar{x}_{1i} - x_1 - \eta_{1i}(t) \tag{5}$$

and [25]

$$\eta_{1i}(t, x_1(t_i)) = e^{-c_1(t-t_i)} \left(\bar{x}_1(t_i) - x_1(t_i)\right) \tag{6}$$

where $c_1 > 0$. In the following, for the sake of simplicity, the dependance on the time interval is dropped, and only the case starting at $t = 0$ is considered, the extension to the different intervals $[t_i, t_{i+1}]$ being trivial. Thus the notation reduces to where,

$$\sigma_1(t, x_1) = \bar{x}_1 - x_1 - \eta_1(t) \tag{7}$$

$$\eta_1(t, x_1(0)) = e^{-c_1 t} \left(\bar{x}_1 - x_1(0)\right) \tag{8}$$

The choice of the exponential term is done in order to have $\sigma_1(0, x_1(0)) = 0$, so that the motion starts on the sliding manifold. Note that this can be done only if the initial value $x_1(0)$ is available, that is not true for the very beginning of the operations. Hence, in practical implementation, an

initialisation phase has to be considered, where the sensors have time to estimate the correct values of all the variables before the control action starts. After this, if the time instant of the reference change is known or estimated in advance, it is possible to compute the exponential terms online. Alternatively, a filtered version of the piecewise-constant reference can be considered, in order to avoid the system state to be pulled off the sliding manifold when discontinuities occur.

The following Lemma is crucial in all the subsequent treatment.

Lemma 1: Consider the first-order ODE

$$\frac{d\xi}{d\lambda} = -\xi + 2 - \frac{\beta(\lambda)}{\xi} \tag{9}$$

where $\lambda \geq 0$, $\beta(\lambda) = \beta_0 + \beta_1 e^{-\mu\lambda}$,

$$\beta_0 < 1, \tag{10}$$

$$\beta_0 + \beta_1 < 1 \tag{11}$$

and $\mu > 0$. Define

$$\Xi_- = 0 \tag{12}$$

if $\beta_0 < 0$, $\beta_0 + \beta_1 < 0$, and

$$\Xi_- = \max\left\{1 - \sqrt{1-\beta_0}, 1 - \sqrt{1-\beta_0-\beta_1}\right\} \tag{13}$$

otherwise. Then (9) has an attractive steady-state

$$\xi_\infty = \lim_{t\to\infty} \xi(t) = 1 + \sqrt{1-\beta_0} \tag{14}$$

and an estimate of the domain of attraction is $\xi > \Xi_-$

Proof: The proof is very simple and can be done graphically by considering the graph of (9) in the plane $(\xi, \dot{\xi})$ at time $t = 0$ and $t = \infty$. ∎

Remark 1: Note that an alternative and less conservative way to study eqn. (9) is to consider the second-order autonomous system

$$\dot{\xi}_1 = -\xi_1 + 2 - \frac{\xi_2 + \beta_0}{\xi_1}, \qquad \xi_1(0) = \xi(0) \tag{15}$$

$$\dot{\xi}_2 = -\mu\xi_2, \qquad \xi_2(0) = \beta_1. \tag{16}$$

Here it is easy to show that the *separatrix* defining the boundary of the basin of attraction of the point $(\xi_\infty, 0)$ is the stable manifold through the point $(1-\sqrt{1-\beta_0}, 0)$. However, there is no simple parameterisation of this curve, so the result of Lemma 1, although more conservative, is more easy to use.

Equipped with the above results, we can now address the problem of controlling the current in the inductor L. The following Theorem addresses this issue.

Theorem 1 (Current tracking): Consider the system (1)–(3), with control law

$$u(t) = \frac{1}{\epsilon}\left(\sigma_1(t, x_1) + \gamma_1 \int_0^t \sigma_1(\tau, x_1) d\tau\right) \tag{17}$$

with σ_1 chosen as in (7), $\gamma_1 > 0$, and ϵ is a "small" positive constant. Define $P_L = E_L\bar{x}_1 + R_L\bar{x}_1^2$, $P_H = E_H^2/R_H$, $P_c = x_3(0)\bar{x}_1$, $P_* = \max(P_L, P_c)$. Moreover, let

$$X_2 = 0 \tag{18}$$

if $|2R_L\bar{x}_1 + E_L| < \sqrt{E_L^2 - 4R_LP_0}$ and $P_0 + P_c < 0$ or

$$X_2 = \frac{E_H}{2}\left(1 - \sqrt{1 - 4\frac{P_0 + P_*}{P_H}}\right) \tag{19}$$

otherwise. Assume that the reference signal $\bar{x}_1$ satisfies

$$\left|2\bar{x}_1 + \frac{E_L}{R_L}\right| < \sqrt{\left(\frac{E_L}{R_L}\right)^2 + \frac{P_H - 4P_0}{R_L}}, \tag{20}$$

that $x_3(0)$ satisfies

$$\bar{x}_1 x_3(0) < \frac{P_H}{4} - P_0 \tag{21}$$

and $x_2(0)$ is such that

$$x_2(0) > X_2. \tag{22}$$

Then the control (17) is such that the closed-loop system is asymptotically stable and, for any $M_1 > 0$, there exists a $T_1 = T_1(\epsilon) > 0$ such that

$$|x_1 - \bar{x}_1(t)| < M_1 + \alpha_1 e^{-\delta_1 t}, \forall t > T_1 \tag{23}$$

where α_1 and δ_1 are suitable positive constants.

Proof: The proof is based on Tikonov's Theorem on the infinite time horizon [26], a well known tool in the Theory of Singularly Perturbed Differential Equations [27]. First, note that the control law (17) is the solution of the differential equation

$$\epsilon\dot{u} = \dot{\sigma_1} + \gamma_1\sigma_1 \tag{24}$$

The above equation shows that the control is the *fast variable* in the set of differential equations (1)–(3), (24). Letting $\epsilon = 0$ in (24), and since $\sigma_1 = 0$ at $t = 0$, $\sigma_1 \equiv 0$ and from $\dot{\sigma}_1 = 0$ the *equivalent control* is obtained

$$u_{eq} = \frac{x_{30} - L\dot{\eta}_1}{x_{20}} \tag{25}$$

where the subscript "0" refers to variables that are computed with $\epsilon = 0$, i.e., the solution of the *reduced order system*

$$\dot{x}_{20} = -\frac{1}{\tau_H}x_{20} - \frac{P_0}{C_H x_{20}} - \frac{1}{C_H}\bar{x}_1 u_{eq} + \nu_H \tag{26}$$

$$\dot{x}_{30} = -\frac{1}{\tau_L}x_{30} + \frac{1}{C_L}\bar{x}_1 + \nu_L \tag{27}$$

For the sake of simplicity, the exponentially decaying term $\eta_1(t)$ is neglected, since it is a design parameter that can be made fast enough so that its presence just slightly modifies the proof. Note that (27) can be easily solved, resulting in

$$x_{30} = (E_L + R_L\bar{x}_1) + [x_3(0) - (E_L + R_L\bar{x}_1)]\, e^{-\frac{t}{\tau_L}}. \tag{28}$$

Replacing (28) in (26) and using the change of coordinates

$$\xi = 2\frac{x_{20}}{E_H}, \quad \lambda = \frac{t}{\tau_H} \tag{29}$$

results into a (normalized) first-order non-autonomous system with the structure (9). Thus, Lemma 1 can be invoked to prove the stability of the reduced-order system. Specifically, eqn. (20) comes from (10) and eqn. (21) from (11), after

denormalization. Next, using Tikonov's Theorem on the infinite time horizon, the proof is completed. ■

Remark 2: Note that condition (10) imposes a bound on the maximum power that the CPL can draw, i.e., $P_0 < \frac{1}{4}\left(\frac{E_L^2}{R_L} + P_H\right)$ However, from (19), positiveness of the radicand imposes a more stringent, bound, namely

$$P_0 < \frac{1}{4}P_H - \max\{P_L, P_c\}. \tag{30}$$

that is reasonable from a physical point of view, since the RHS is the maximum power that both sources can supply to the network.

Remark 3: Lemma 1 can be used also to compute the steady-state value of the voltage x_{20}, that is

$$x_{20ss} = \frac{E_H}{2} + \sqrt{\left(\frac{E_H}{2}\right)^2 - (P_0 + P_L)R_H} \tag{31}$$

Remark 4: Note that the control strategy in Theorem 1 produces a continuous control law. In order to be implemented on a switching system, with a binary control $u \in \{0, 1\}$ the further assumption $0 \leq u_{eq} \leq 1$ has to be checked. Incidentally, note that this condition is also necessary to implement a VSC strategy [28]. If this assumption holds, the high gain term $1/\epsilon$ can be replaced by a Heaviside function, possibly with a small hysteresis, or a $\Sigma - \Delta$ modulator [29] can be employed.

B. Current control, HV side

As stated in the Introduction, the second control objective is to limit the current supplied by the generator in the case of generator overload. In principle, since the generator current and the voltage on the HV capacitor are related by

$$I_g = \frac{E_H - x_2}{R_H} \tag{32}$$

imposing a fixed value I_{OL} to the generator current translates into selecting the following set-point for x_2

$$\bar{x}_2 = E_H - R_H I_{OL} \tag{33}$$

However, defining a sliding manifold directly on the HV-side capacitor is not viable, since the resulting control action is not stabilizing, due to an unstable zero-dynamics [24]. For this reason, an indirect feedback action has been chosen, namely, first a suitable reference for the inductor current is selected adaptively, based on the HV voltage error, then Theorem 1 is used again to track this reference. The following Theorem formalises this issue.

Theorem 2 (Adaptive current reference): Consider the system (1)–(3), with control law defined in Theorem 1, assuming that all the hypotheses of Theorem 1 hold. Let

$$\sigma_2(t, x_2) = \bar{x}_2 - x_2 - \eta_2(t) \tag{34}$$

with

$$\eta_2(t, x_2(0)) = e^{-c_2 t}\left(\bar{x}_2(0) - x_2(0)\right) \tag{35}$$

where $c_2 > 0$, and let the reference current $\bar{x}_1$ be

$$\bar{x}_1(t) = -\frac{1}{\epsilon}\int_0^t \sigma_2(\tau, x_2(\tau))d\tau \tag{36}$$

Assume $x_1(0) > 0$ and $x_2(0) > 0$. Then the closed loop system is asymptotically stable and such that, for any $M_2 > 0$, there exists a $T_2 = T_2(\epsilon) > 0$ such that

$$|x_2 - \bar{x}_2| < M_2 + \alpha_2 e^{-\delta_2 t}, \forall t > T_2 \tag{37}$$

where α_2 and δ_2 are suitable positive constants.

Proof: Also in this Theorem the proof is based on the theory of Singular Perturbations. Again, we neglect the exponentially decaying term. First, note that the reference current (36) can be obtained from

$$\dot{\bar{x}}_1 = -v \tag{38}$$

$$\epsilon\dot{v} = \dot{\sigma}_2 \tag{39}$$

Considering (24), the *fast dynamic* of the whole system in the fast time scale is given by

$$\epsilon\begin{pmatrix} \dot{u} \\ \dot{v} \end{pmatrix} = \begin{pmatrix} -\frac{1}{L}x_2(0) & -1 \\ \frac{1}{C_H}x_1(0) & 0 \end{pmatrix}\begin{pmatrix} u \\ v \end{pmatrix} + \text{constant terms} \tag{40}$$

So, due to the hypotheses $x_1(0) > 0$, $x_2(0) > 0$, the fast dynamics is stable.

Stability of the reduced order system, with $\sigma_1 = 0$ and $\sigma_2 = 0$ is easily proved since the reduced order system is simply

$$\dot{x}_{30} = -\frac{1}{\tau_L}x_{30} + \frac{1}{C_L}\bar{x}_{10} + \nu_L \tag{41}$$

$$\dot{\bar{x}}_{10} = 0 \tag{42}$$

Note that the last equation implies that $\bar{x}_{10}$ is constant, then the rest of the proof is similar to that of Theorem 1. ■

Remark 5: Note that the assumptions $x_2(0) > 0$ and $x_1(0) > 0$ in Theorem 2 are not conservative. The first one is obvious from a physical point of view, while the second is obvious during standard operations of the converter, since the overload phase always starts when the battery is charging.

C. Supervisor Design

The above results can be used to define a supervisory controller. The controller encompasses two operational modes, as follows

- in normal operating conditions (Mode 1), the generator on the high voltage side recharges the battery, exploiting the current set-point tracking in Theorem 1.
- if a new load requires power so that an overload occurs the supervisor must commute to generator current limitation mode (Mode 2), and Theorem 2 is used to define a new current profile to track.

This behaviour can be described by a simple automaton that comprises just two modes. Care must be given at each commutation, checking if the current state of the converter is within the ROA of the next mode. Otherwise, the supervisor must prevent mode change. In order to avoid chattering between the two modes, for practical implementation an hysteresis with band $[I_{OL} - \theta, I_{OL} + \theta]$ is used rather than a strict threshold. Actually, in order to ensure stability of the switched system two conditions have to be tested: first, the commutation must take place only when the state of

the converter before the commutation is in the ROA of the closed-loop after the commutation; second, there should be some function related to the system energy (Lyapunov-like functions) that do not increase between analogous commutations [21], i.e., each time a commutation from Mode 1 to Mode 2 happens, the value of the Lyapunov-like function must be monotonically nonicreasing (the same for the commutation from Mode 2 to Mode 1), so that the overall commutation is contractive. As an alternative criterion for contraction, it is possible to impose a minimum dwell-time that must elapse before a new commutation is enabled [30]. A detailed derivation of this dwell-time is still under investigation. In this paper it is assumed that the occurrence of load variation and the fast dynamic of the electronic components are such that the dwell time has elapsed between consecutive load changes. Moreover, also the definition of the hysteresis band θ given above has the effect of introducing a minimum dwell-time.

IV. SIMULATION RESULTS

The controller strategy defined in Section III has been tested on a BBCU in two different scenarios. Specifically, Scenario 1 presents the power grid as in Fig. 1, where the HV side is connected to a battery through a BBCU converter. In Scenario 2 instead, two parallel BBCU converters are considered, each of which controlled by the respective low level controller. The power grid has been designed using the parameters of Table I.

TABLE I
BBCU DATA

E_L	28	[V]
E_H	270	[V]
L	10	[mH]
C_H	800	[μF]
C_L	400	[μF]
R_H	100	[mΩ]
R_L	100	[mΩ]
P_{01}	100	[W]
P_{02}	4200	[W]
P_{03}	4600	[W]

The controller parameters are $\gamma_1 = 1$, $c_1 = c_2 = 100$, $\epsilon = 10^{-3}$ where the subscript identifies the BBCU converter connected to the grid. With the above parameters all the inequalities in Section III are satisfied. Specifically, by using (22), the ROA is the interval $x_2 > 0.144$V. Moreover, a first order filter

$$F(s) = \frac{1}{\tau_g s + 1} \tag{43}$$

with $\tau_g = 0.01$s is considerer to filter the generator current in the switching implementation. A detailed MATLAB/SimPowerSystem simulator (Fig. 2) has been designed to perform detailed simulations. The switching implementation is operated by a PWM modulator with switching frequency 200kHz.

In both scenarios a piecewise constant CPL is considered. More precisely, CPL variations occur at time instants 2s, 4s and 6s as shown in Fig. 3.

Scenario 1 will be considered first. Initially, a CPL with power demand to P_{01} is connected to the grid. As apparent in Fig. 4 the controller charges the battery with constant current $\bar{x}_1 = 10$A. Then, at $t = 2$s, a CPL variation occurs that takes the power demand equal to P_{02}. This load variation causes an overload (see Fig. 5) and the second mode starts. Note how in overload mode, after a short transient, the controller drives the generator current to the constant value $I_{OL} = 16$A. However, the new load is such that the battery can be still charged with a reduced current. The next load variation, that takes the CPL value to P_{03} at $t = 4$s, is such that the generator alone cannot supply the loads, hence the battery helps the generator in feeding the load, as shown by the negative current in the inductor. Finally, at $t = 6$s the initial conditions are restored, and the supervisor goes back to Mode 1 setting the inductor current to the set point $\bar{x}_1 = 10$A.

The equivalent control is shown in Figure 6, and is shown to be well within the interval $[0, 1]$. As stated above, Scenario 2 is more complex, since also a controlled BBCU is inserted in the grid, acting as another CPL. The CPL variation profile is the same as considered in Scenario 1 and the obtained simulation results are shown in Figs 7–9. Two different inductor current set points are considered for the BBCU converters, respectively 10A and 5A as evident in Fig. 7. It is worth noting how, when in overload mode, the current flowing from the batteries to the CPL is equally provided by the two converters (Fig. 7 between 2s and 6s). As Fig. 9 shows, also in Scenario 2, the equivalent controls of both controllers are always in the interval $[0, 1]$.

V. CONCLUSIONS

In this paper a two layers control strategy has been presented for the intelligent control of a BBCU bidirectional converter regulating the energy flow to feed a CPL for aeronautic applications. The two layers have been designed as follow. The higher level (supervisory level) is in charge of imposing a set-point for the inductor current to either charge the battery or turn the battery into a further power source in order to feed the load. When in overload mode, the supervisor imposes the generator current to a limit value as well. The lower level is in charge of regulating the BBCU switching frequency in order to reach the prescribed time-varying inductor current. Stability of the low level control has been proved resorting the Theory of Singularly Perturbed Differential Equations and the definition of a Sliding Manifold. The supervisor has been implemented as a finite-state automaton. Simulation results, obtained on a detailed MATLAB/Simulink simulator, resulting from two different topological and operating scenarios, are presented in order to show the effectiveness of the proposed strategy.

REFERENCES

[1] [Online]. Available: www.moreelectricaircraft.com

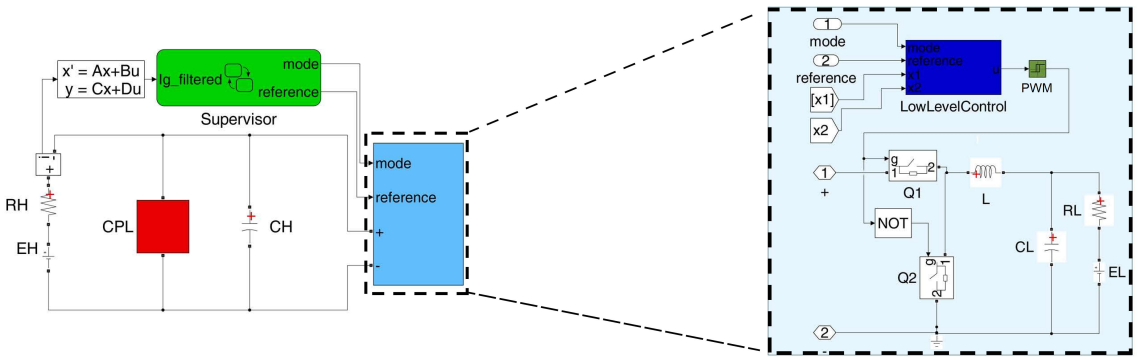

Fig. 2. SimPowerSystem simulation scheme

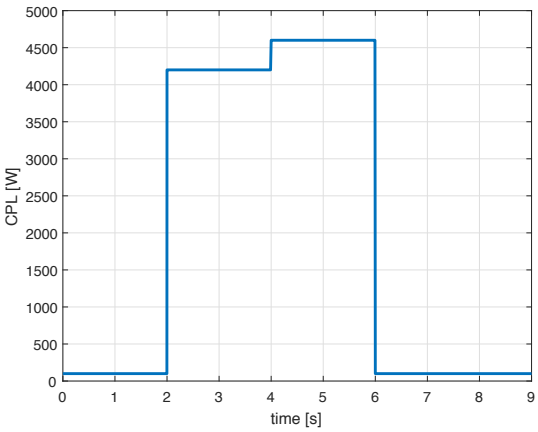

Fig. 3. CPL variation

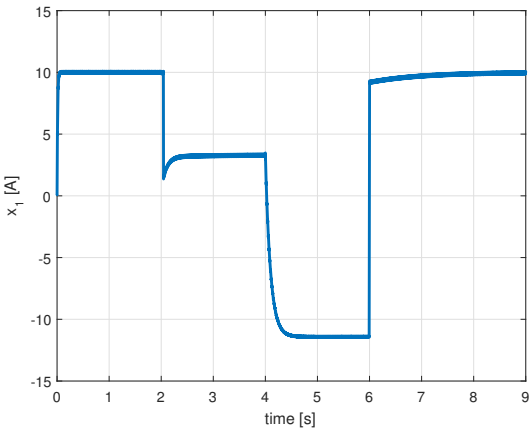

Fig. 4. Inductor current, Scenario 1

[2] (2002-2005) Poa-research project works to optimise aircraft power use. [Online]. Available: https://cordis.europa.eu/project/rcn/60125_en.html

[3] (2006-2009) Moet-more open electrical technologies. [Online]. Available: http://ec.europa.eu/research/transport/projects/items/moet_en.htm

[4] (2010-2015) Clean sky at a glance. [Online]. Available: http://www.cleansky.eu/content/document/clean-sky-glance-0

[5] H. Huang. (2015) Challanges in more electric aircraft (mea). Internet newsletter. IEEE Transportation Electrification Community. [Online]. Available: https://tec.ieee.org/newsletter/july-august-2015/challenges-in-more-electric-aircraft-mea

[6] G. Canciello, A. Cavallo, and B. Guida, "Robust control of aeronautical electrical generators for energy management applications," *International Journal of Aerospace Engineering*, vol. 2017, 2017.

[7] ——, "Control of energy storage systems for aeronautic applications," *Journal of Control Science and Engineering*, vol. 2017, 2017.

[8] J. A. Barrado, A. E. Aroudi, H. Valderrama-Blavi, J. Calvente, and L. Martinez-Salamero, "Analysis of a self-oscillating bidirectional dcdc converter in battery energy storage applications," *IEEE Transactions on Power Delivery*, vol. 27, no. 3, pp. 1292–1300, July 2012.

[9] A. Cavallo, G. Canciello, and B. Guida, "Supervised control of buck-boost converters for aeronautical applications," *Automatica*, vol. 83, pp. 73–80, 2017.

[10] A. Cavallo, B. Guida, A. Buonanno, and E. Sparaco, "Smart buck-boost converter unit operations for aeronautical applications," in *2015 54th IEEE Conference on Decision and Control (CDC)*, Dec 2015, pp. 4734–4739.

[11] G. S., *Electrical Machines, Second Ed.* Pearson Education, 2012.

[12] L. Rubino, B. Guida, F. Liccardo, P. Marino, and A. Cavallo, "Buck-boost dc/dc converter for aeronautical applications," in *Industrial Electronics (ISIE), 2010 IEEE International Symposium on*, july 2010, pp. 2690 –2695.

[13] B. Guida and A. Cavallo, "Supervised bidirectional dc/dc converter for intelligent fuel cell vehicles energy management," in *IEEE International Electric Vehicle Conference 2012*, march 2012.

[14] A. Cavallo, G. Canciello, and B. Guida, "Supervisory control of dcdc bidirectional converter for advanced aeronautic applications," *International Journal of Robust and Nonlinear Control*, vol. 28, no. 1, pp. 1–15, 2018. [Online]. Available: https://onlinelibrary.wiley.com/doi/abs/10.1002/rnc.3851

[15] A. B. Jusoh, "The instability effect of constant power loads," in *PECon 2004. Proceedings. National Power and Energy Conference, 2004.*, Nov 2004, pp. 175–179.

[16] A. Emadi, A. Khaligh, C. H. Rivetta, and G. A. Williamson, "Constant power loads and negative impedance instability in automotive systems: definition, modeling, stability, and control of power electronic converters and motor drives," *IEEE Transactions on Vehicular Technology*, vol. 55, no. 4, pp. 1112–1125, July 2006.

[17] X. Liu, Y. Zhou, W. Zhang, and S. Ma, "Stability criteria for constant power loads with multistage *lc* filters," *IEEE Transactions on Vehicular Technology*, vol. 60, no. 5, pp. 2042–2049, Jun 2011.

[18] B. A. Martnez-Trevio, R. Jammes, A. E. Aroudi, and L. Martnez-Salamero, "Sliding-mode control of a boost converter supplying a constant power load," *IFAC-PapersOnLine*, vol. 50, no. 1, pp. 7807 – 7812, 2017, 20th IFAC World Congress. [Online]. Available: http://www.sciencedirect.com/science/article/pii/S2405896317315410

[19] F. Gao and S. Bozhko, "Modeling and impedance analysis of a single dc bus-based multiple-source multiple-load electrical power system," *IEEE Transactions on Transportation Electrification*, vol. 2, no. 3, pp. 335–346, Sept 2016.

[20] M. K. AL-Nussairi, R. Bayindir, S. Padmanaban, L. Mihet-Popa, and P. Siano, "Constant power loads (cpl) with microgrids: Problem definition, stability analysis and compensation techniques," *Energies*, vol. 10, no. 10, 2017. [Online]. Available: http://www.mdpi.com/1996-1073/10/10/1656

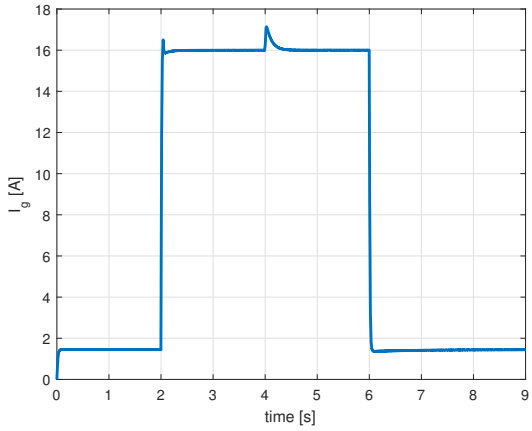

Fig. 5. Generator current, Scenario 1

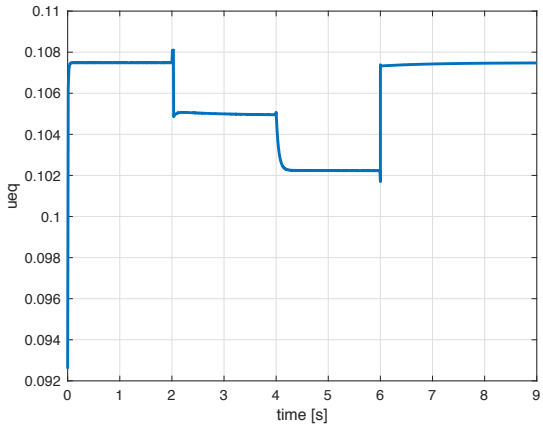

Fig. 6. Equivalent control, Scenario 1

[21] M. S. Branicky, "Multiple lyapunov functions and other analysis tools for switched and hybrid systems," *IEEE Transactions on Automatic Control*, vol. 43, no. 4, pp. 475–482, Apr 1998.

[22] M. M. Tousi, I. Karuei, S. Hashtrudi-Zad, and A. G. Aghdam, "Supervisory control of switching control systems," *Systems & Control Letters*, vol. 57, no. 2, pp. 132 – 141, 2008. [Online]. Available: http://www.sciencedirect.com/science/article/pii/S0167691107001077

[23] P. J. Ramadge and W. M. Wonham, "Supervisory control of a class of discrete event processes," *SIAM J. Control Optim.*, vol. 25, no. 1, pp. 206–230, Jan. 1987. [Online]. Available: http://dx.doi.org/10.1137/0325013

[24] A. Cavallo and B. Guida, "Sliding mode control for dc/dc converters," in *Decision and Control (CDC), 2012 IEEE 51st Annual Conference on*, Dec 2012, pp. 7088–7094.

[25] A. Cavallo, G. de Maria, and P. Nistri, "Robust control design with integral action and limited rate control," *Automatic Control, IEEE Transactions on*, vol. 44, no. 8, pp. 1569–1572, Aug 1999.

[26] F. Hoppenstead, "Singular perturbations on the infinite time interval," *Trans. Am. Math. Soc.*, vol. 123, pp. 521–535, 1966.

[27] H. Khalil, *Nonlinear Systems, Third Edition*. Prentice Hall, 2002.

[28] H. Sira-Ramirez, "Sliding motions in bilinear switched networks," *IEEE Trans. on Circuits axfnd Systems*, vol. 34, pp. 919–933, 1987.

[29] H. Sira-Ramirez and R. Silva-Ortigoza, *Control Design Techniques in Power Electronic Devices*, ser. Power Systems. Springer, 2006.

[30] H. Lin and P. J. Antsaklis, "Stability and stabilizability of switched linear systems: A survey of recent results," *IEEE Transactions on Automatic Control*, vol. 54, no. 2, pp. 308–322, Feb 2009.

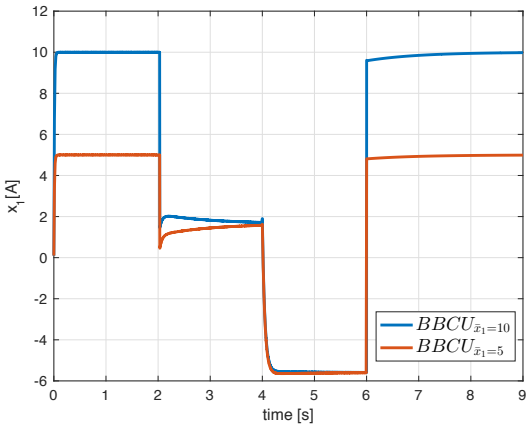

Fig. 7. Inductor current, Scenario 2

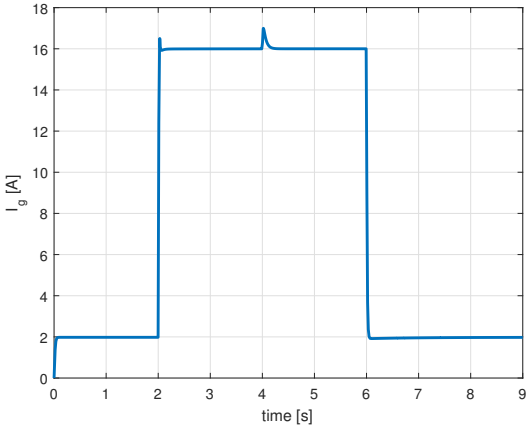

Fig. 8. Generator current, Scenario 2

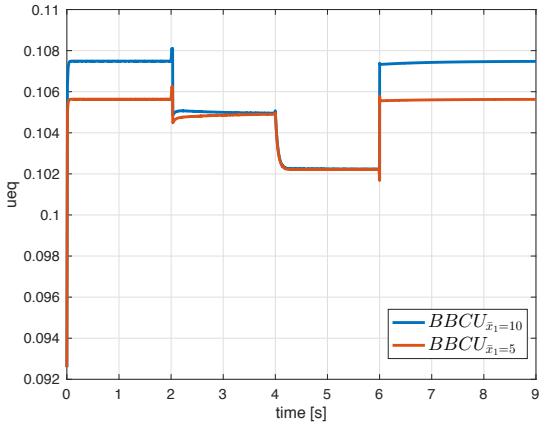

Fig. 9. Equivalent control, Scenario 2